

# Universal Ti-rich termination of atomically flat SrTiO<sub>3</sub> (001), (110), and (111) surfaces

A. Biswas,<sup>1</sup> P. B. Rossen,<sup>2</sup> C.-H. Yang,<sup>3,a)</sup> W. Siemons,<sup>4</sup> M.-H. Jung,<sup>1</sup> I. K. Yang,<sup>1</sup> R. Ramesh,<sup>2,4,5</sup> and Y. H. Jeong<sup>1,a)</sup>

<sup>1</sup>Department of Physics, Pohang University of Science and Technology, Pohang 790-784, Republic of Korea

<sup>2</sup>Department of Materials Science and Engineering, University of California, Berkeley, California 94720, USA

<sup>3</sup>Department of Physics and Institute for the NanoCentury, KAIST, Daejeon 305-701, Republic of Korea

<sup>4</sup>Department of Physics, University of California, Berkeley, California 94720, USA

<sup>5</sup>Materials Science Division, Lawrence Berkeley National Laboratory, Berkeley, California 94720, USA

(Received 12 October 2010; accepted 10 January 2011; published online 31 January 2011)

We have studied the surface termination of atomically flat SrTiO<sub>3</sub> surfaces treated by chemical etching and subsequent thermal annealing, for all commercially available orientations (001), (110), and (111). Atomic force microscopy confirms that our treatment processes produce unit cell steps with flat terrace structures. We have also determined the topmost atomic layer of SrTiO<sub>3</sub> surfaces through time-of-flight mass spectroscopy. We found that all three orientations exhibit a Ti-rich surface. Our observation opens doors for interface engineering along the [110] and [111] directions in addition to a well known [100] case, which widens the range of functional heterostructures and interfaces. © 2011 American Institute of Physics. [doi:10.1063/1.3549860]

Strontium titanate (SrTiO<sub>3</sub>, STO) has received special attention as a substrate onto which many perovskite compounds have been synthesized. STO is a paraelectric insulator and has a cubic perovskite structure with a lattice parameter of 3.905 Å at room temperature, which makes it suitable to grow many perovskites by offering good lattice mismatch. A layer-by-layer growth on atomically flat single-terminated STO (111) would allow the synthesis of B-site ordered double perovskites theoretically proposed.<sup>1,2</sup>

In order to fabricate superlattices and functional interfaces with atomic precision, atomically flat substrates with a known and homogeneous termination are required. In order to achieve this, surface treatments and analyses have been studied extensively. Preparation of a well-defined atomically flat surface of STO (001) started in the 1990s by Kawasaki *et al.*<sup>3</sup> and was later refined by Koster *et al.*<sup>4</sup> These authors introduced the chemical and thermal treatment to get atomically flat STO (001) surfaces and confirmed, with ion scattering, that the surface is TiO<sub>2</sub> terminated. Recent first-principles studies have investigated surface relaxation on the STO (001) and STO (110) surfaces.<sup>5,6</sup> It has also been reported that SrO termination on STO (001) can be stabilized by growing STO on NdGaO<sub>3</sub> (110) substrates,<sup>7</sup> as well as annealing the STO (001) substrates at temperatures higher than 1300 °C.<sup>8</sup> A variety of surface reconstructions, (2 × 1), (2 × 2) on (001),<sup>9–11</sup> (1 × 1), (3 × 1) on (110),<sup>12,13</sup> and (1 × 1) on (111)<sup>14,15</sup> surfaces have been studied.

Atomically flat (110) and (111) STO surfaces with a step terrace structure have not been available until recently, when new treatment methods were reported using annealing in an oxygen environment.<sup>16,17</sup> To the best of our knowledge, there is no experimental evidence of the termination of either the (110) or the (111) atomically flat surfaces to this date. In this report we present atomically flat surfaces of which single surface termination along (001), (110), and (111) orientation is identified by time-of-flight mass spectroscopy (TOF-MS).

The STO (001) crystal structure consists of alternating layers of a charge neutral SrO layer and a charge neutral TiO<sub>2</sub> layer [Fig. 1(a)] with a step height of  $d_{001}=3.905$  Å. STO (001) is known to have a nonpolar TiO<sub>2</sub> termination, which is very stable in terms of surface energy, and the treatment technique to get the single termination has been well established. The STO (110) crystal structure can be expressed by stacking of alternating SrTiO<sup>4+</sup> and O<sub>2</sub><sup>4-</sup> layers [Fig. 1(b)]. The step height in this case corresponds to  $d_{110}=2.76$  Å. In the ideal perovskite crystal structure the surface would be terminated by either a SrTiO<sup>4+</sup> layer or an O<sub>2</sub><sup>4-</sup> layer. The STO (111) crystal structure contains alternately stacking of two hexagonal surface structures of SrO<sub>3</sub><sup>4-</sup> and Ti<sup>4+</sup> as shown in Fig. 1(c). The distance between adjacent Ti<sup>4+</sup> and SrO<sub>3</sub><sup>4-</sup> layers is  $d_{111}=2.25$  Å.

The studied STO (001), (110), and (111) substrates have a low miscut angle ( $\theta < 0.1^\circ$ ) and were supplied by CrysTec GmbH. In order to get a well-defined surface in terms of morphology and termination, we carried out chemical etch-

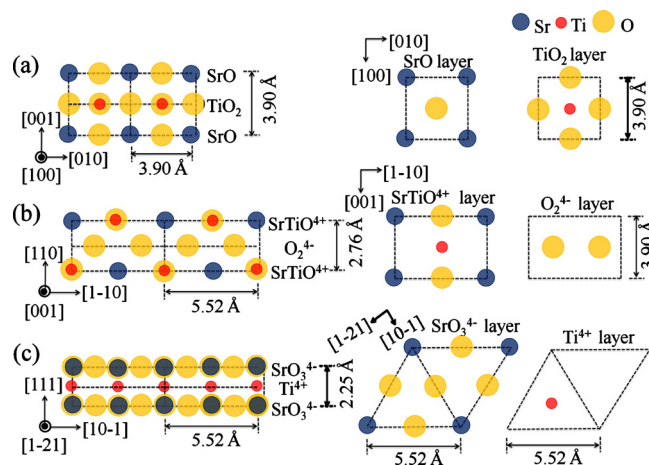


FIG. 1. (Color online) Schematic representation of cross-sectional crystal structures (left panel) and two possible ideal termination layers (right panel) from a crystallographic point of view for (001), (110), and (111) orientated SrTiO<sub>3</sub> substrates.

<sup>a)</sup>Authors to whom correspondence should be addressed. Electronic addresses: chyang@kaist.ac.kr and yhj@postech.ac.kr.

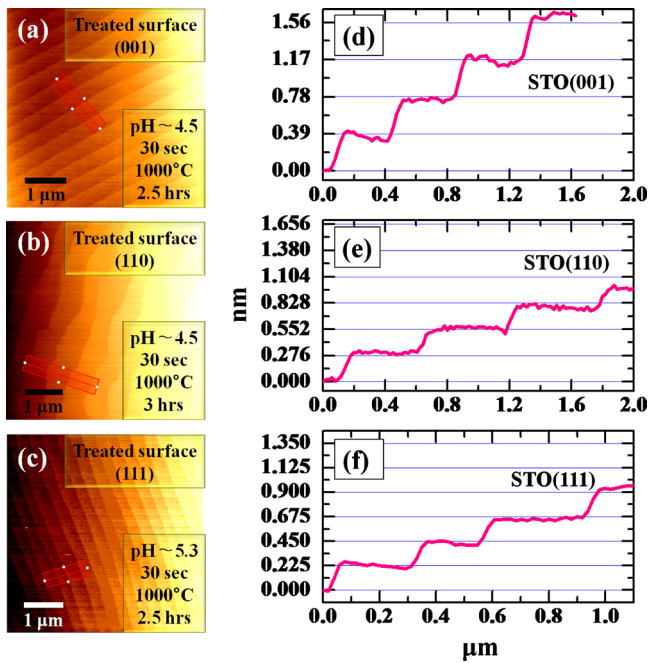


FIG. 2. (Color online) (a)–(c) show representative surface morphology of the treated (001), (110), and (111) surfaces; the conditions of chemical etching and thermal annealing are expressed in the inset of the figures. On right side is plotted the cross-sectional profile showing the step height. The distance between two horizontal guide lines corresponds to the lattice spacing expected in single-layer-step for each crystal orientation; 0.39 nm for (001), 0.276 nm for (110), and 0.225 nm for (111) surface shown in (d), (e), and (f) respectively.

ing and thermal annealing in an oxygen environment. First, we cleaned the substrates with acetone and methanol, respectively, for 10 min and performed ultrasonic soaking in de-ionized water for 5 min. Then we etched the surfaces in a buffered hydrogen fluoride ( $\text{NH}_4\text{F}:\text{HF}=7:1$ ) solution for 30 s. We adjusted the potential of hydrogen (pH) of the etching solution, by diluting it with de-ionized water, to pH = 4.5 for (100) and (110) substrates and pH = 5.3 for (111) substrates. The pH of the solutions was confirmed by an Orion 3 Star pH benchtop meter. Strontium oxide reacts stronger with water than titanium oxide, forming strontium hydroxides, which easily dissolve in the etching solution.<sup>4</sup> After completing the etching for 30 s, we annealed the substrates at 1000 °C in an oxygen gas flow for 2–3 h to get a step terrace structure; the annealing temperature was selected to avoid Sr diffusion from the bulk.<sup>8</sup> The combination of etching and the annealing leads to atomic reorganization on the surface. Through this treatment, the surfaces become atomically flat and exhibit clear step terrace structures with a sharp straight line at step edges having the theoretically expected single unit cell height (see Fig. 2).

In order to determine the topmost atomic layer of the STO (001), STO (110), and STO (111) surfaces, we performed TOF-MS (Ionwerks, Inc.) which is capable of high sensitive surface composition analysis with isotope resolution.<sup>18–20</sup> Figure 3(a) shows the experimental configuration; pulsed potassium ions ( $^{39}\text{K}$ ) with a kinetic energy of 10 keV are projected at the surface of the substrates at an incident angle of 15°, and recoiled ions from the sample are collected at a recoiling angle of 60° through the mass spectroscopy of recoiled ions (MSRI). Since heavy elements fly slower, the measured TOF can be converted to the atomic mass of the recoiled ion. The intensities of recoiled ions are

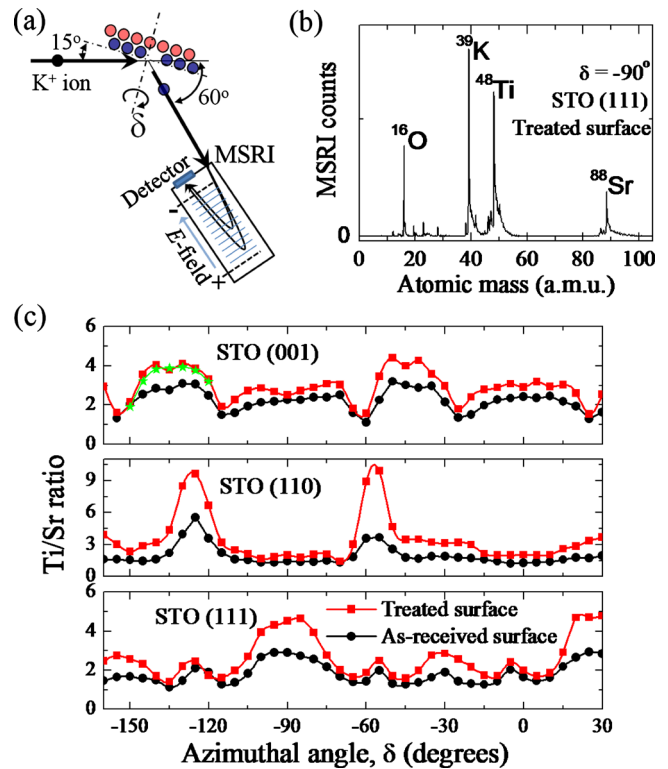


FIG. 3. (Color online) (a) Experimental configuration of TOF-MS. (b) A representative spectrum obtained from the chemically treated surface in which peaks are allocated to  $^{88}\text{Sr}$ ,  $^{48}\text{Ti}$ ,  $^{16}\text{O}$ , and  $^{39}\text{K}$  ions. (c) The ratio of Ti recoiled ions with respect to Sr recoiled ions is plotted as a function of the azimuthal angle, comparing the treated surface to the as-received one. The treated surfaces of all three orientations have a higher Ti/Sr ratio. Two different samples with treated (001) surface show nearly the same results (compare stars symbols with square symbols in the top panel), which indicates that the Ti/Sr ratio of the as-received and treated substrates is meaningfully different.

strongly influenced by neighboring ions surrounding the recoiled ions on the surface as a result of blocking or/and shadowing effects. Therefore, systematic investigations on the azimuthal angle ( $\delta$ ) dependence of the MSRI counts can reveal in-plane crystalline structures.

All the measurements were conducted in high vacuum at 150 °C. Before measurements, the substrates were annealed at 600 °C in 100 mTorr of oxygen gas in order to remove hydrocarbon contaminations. The value of the azimuthal angle ( $\delta$ ) was defined to be zero when the projected direction of the incident ions on the surface is parallel to the in-plane crystalline axis of [100], [1–10], and [1–10] for each (001), (110), and (111) surface, respectively. In Fig. 3(b) a representative MSRI spectrum for the chemically treated surface with clear step edges is presented. Strontium, titanium, and oxygen recoiled ions are detected as well as scattered potassium ions. The numbers of recoiled ions to reach the detector at a certain scattering geometry are obtained from the integration of the peak area in the spectrum. In Fig. 3(c), we show the intensity of Ti ions with respect to Sr ions as a function of the azimuthal angle for both as-received and treated surfaces of (001), (110), and (111) STO substrates. From this it is clear that the Ti-rich layer becomes dominant by the chemical and thermal treatment for each surface orientation. In combination with the AFM images, the TOF-MS results lead us to a conclusion that all three surfaces become homogeneous Ti-rich termination by the treatment.

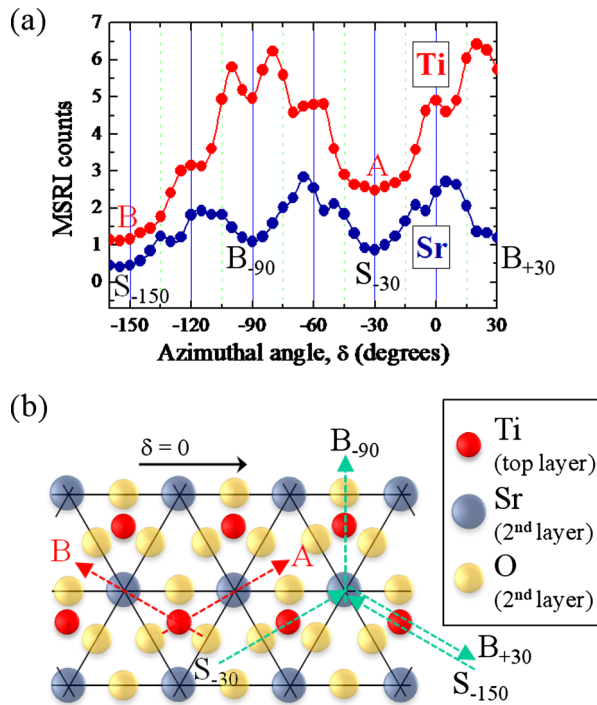


FIG. 4. (Color online) (a) Azimuthal angle ( $\delta$ ) scan of MSRI for Ti ions and Sr ions on the treated (111) surface. (b) Schematic of ionic arrangement on the (111) surfaces is shown. The dashed arrows indicate the projected direction toward the MSRI detector. Ti recoiled ions toward A or B direction are blocked by neighboring Sr ions. On the other hand, Sr recoiled ions toward  $\delta = -90^\circ$  and  $\delta = +30^\circ$  are blocked by neighboring Ti ions. The MSRI intensity of Sr ions can be reduced additionally by shadowing effect along  $\delta = -30^\circ$  and  $\delta = -150^\circ$ . The blocking/shadowing of oxygen ions and next-nearest ions would be secondary effect to produce fine structures in the spectra.

It is worthwhile to mention that in reality the (110) surface is not as simple as we considered in Fig. 1(b) because the ideal crystal structure is made of alternating  $\text{SrTiO}^{4+}$  and  $\text{O}_2^{4-}$  layers. The coexistence of Sr and Ti ions on the same plane contradicts the observation of the Ti ion enhancement by the treatment in the MSRI spectrum, which probably indicates that more sophisticated surface reconstruction should be considered. In this regard, a theoretical work using density functional theory supports our experimental observation and predicts that  $\text{TiO}^{2+}$  surface where  $\text{Sr}^{2+}$  ions are missing is the most stable among five candidates ( $\text{SrTiO}^{4+}$ ,  $\text{O}_2^{4-}$ ,  $\text{Sr}^{2+}$ ,  $\text{TiO}^{2+}$ , and  $\text{O}^{2-}$ ).<sup>12</sup> This prediction is intuitively reasonable in terms of two points: (i) the missing of  $\text{Sr}^{2+}$  ions reduces the high polarity at the surface, possibly decreasing surface energy, and (ii) the chemical treatment tends to remove Sr ions on the surface.

The Ti-layer termination of the (111) treated surface is also supported by analysis of the azimuthal angle dependence of Ti and Sr MSRI as shown in Fig. 4. The decrease of the recoiled ions at specific azimuthal angles is due to either blocking effect or shadowing effect. The blocking effect refers to a situation where a neighboring ion blocks the recoiled ion traveling to the MSRI detector, whereas the shadowing effect means that a neighboring ion screens the incident potassium ions before scattering.<sup>18</sup> The ions at the topmost layer are not associated with the shadowing effect unless the potassium ions are incident at small grazing angle. However, ions at the second layer can be prevented to be recoiled by shadowing of a certain ion on the top. Both Ti and Sr ions on the (111) surface are threefold symmetric as

displayed in Fig. 4(b). If we considered only blocking effect, the MSRI of both ions should have shown threefold symmetric behavior along the azimuthal rotation. However the MSRI of Sr ions turns out to have a large dip every  $60^\circ$  azimuthal rotation because of the shadowing effect, indicating that the Ti layer is the topmost layer and the layer including Sr ions is underneath. Unfortunately the (110) and (001) cases are not straightforward because the Sr and Ti ions on the surfaces are twofold or fourfold symmetric. In this case, the shadowing effect happens at the same azimuthal angles where the blocking effect appears.

In summary, we have prepared atomically flat STO (001), (110), and (111) surfaces with a clear step terrace structure by selective etching with a buffered HF solution and thermal annealing. Using TOF-MS measurements, we have identified the topmost layer as Ti-rich for all three cases, i.e., a  $\text{TiO}_2$  layer for the (001) surface, probably a Sr-deficient  $\text{TiO}$  layer for the (110) surface, and a Ti layer for the (111) surface. However, the structural details of the treated (110) surface still need to be uncovered. The present work provides a basis to explore new artificial superlattices or multilayers and new functional interfaces along the [110] and [111] directions in addition to the [001] direction.

C.-H.Y. and Y.H.J. acknowledge the support by the National Research Foundation of Korea (NRF) funded by the Ministry of Education, Science and Technology, Korea (Contract Nos. 2010-0013528 and 2010-0014523). W.S. acknowledges the Dutch Organization for Scientific Research (NWO-Rubicon).

- <sup>1</sup>P. Baettig and N. A. Spaldin, *Appl. Phys. Lett.* **86**, 012505 (2005).
- <sup>2</sup>S. Takagi, A. Subedi, V. R. Cooper, and D. J. Singh, *Phys. Rev. B* **82**, 134108 (2010).
- <sup>3</sup>M. Kawasaki, K. Takahashi, T. Maeda, R. Tsuchiya, M. Shinohada, O. Ishiyama, T. Yonezawa, M. Yoshimoto, and H. Koinuma, *Science* **266**, 1540 (1994).
- <sup>4</sup>G. Koster, B. L. Kropman, G. J. H. M. Rijnders, D. H. A. Blank, and H. Rogalla, *Appl. Phys. Lett.* **73**, 2920 (1998).
- <sup>5</sup>R. I. Eglitis and D. Vanderbilt, *Phys. Rev. B* **77**, 195408 (2008).
- <sup>6</sup>E. Heifets, W. A. Goddard III, E. A. Kotomin, R. I. Eglitis, and G. Borstel, *Phys. Rev. B* **69**, 035408 (2004).
- <sup>7</sup>M. Radovic, N. Lampis, F. Miletto Granozio, P. Perna, Z. Ristic, M. Saluzzo, C. M. Schlepütz, and U. Scotti di Uccio, *Appl. Phys. Lett.* **94**, 022901 (2009).
- <sup>8</sup>R. Bachelet, F. Sánchez, F. J. Palomares, C. Ocal, and J. Fontcuberta, *Appl. Phys. Lett.* **95**, 141915 (2009).
- <sup>9</sup>N. Erdman, K. R. Poepelmeier, M. Asta, O. Warschkow, D. E. Ellis, and L. D. Marks, *Nature (London)* **419**, 55 (2002).
- <sup>10</sup>R. Herger, P. R. Willmott, O. Bunk, C. M. Schlepütz, B. D. Patterson, and B. Delley, *Phys. Rev. Lett.* **98**, 076102 (2007).
- <sup>11</sup>R. Herger, P. R. Willmott, O. Bunk, C. M. Schlepütz, B. D. Patterson, B. Delley, V. L. Shneerson, P. F. Lynn, and D. K. Saldin, *Phys. Rev. B* **76**, 195435 (2007).
- <sup>12</sup>F. Bottin, F. Finocchi, and C. Noguera, *Phys. Rev. B* **68**, 035418 (2003).
- <sup>13</sup>J. A. Enterkin, A. K. Subramanian, B. C. Russell, M. R. Castell, K. R. Poepelmeier, and L. D. Marks, *Nature Mater.* **9**, 245 (2010).
- <sup>14</sup>A. Pojani, F. Finocchi, and C. Noguera, *Surf. Sci.* **442**, 179 (1999).
- <sup>15</sup>L. D. Marks, A. N. Chiamonti, F. Trans, and P. Blaha, *Surf. Sci.* **603**, 2179 (2009).
- <sup>16</sup>Y. Mukunoki, N. Nakagawa, T. Susaki, and H. Y. Hwang, *Appl. Phys. Lett.* **86**, 171908 (2005).
- <sup>17</sup>J. Chang, Y. S. Park, and S. K. Kim, *Appl. Phys. Lett.* **92**, 152910 (2008).
- <sup>18</sup>J. Wayne Rabalais, *Principles and Applications of Ion Scattering Spectroscopy* (Wiley, Hoboken, NJ, 2003).
- <sup>19</sup>O. Auciello, A. R. Krauss, J. Im, and J. A. Schultz, *Annu. Rev. Mater. Sci.* **28**, 375 (1998).
- <sup>20</sup>J. E. Kleibecker, G. Koster, W. Siemons, D. Dubbink, B. Kuiper, J. L. Blok, C.-H. Yang, J. Ravichandran, R. Ramesh, J. E. ten Elshof, D. H. A. Blank, and G. Rijnders, *Adv. Funct. Mater.* **20**, 3490 (2010).